Chapter 7

Oxygen Isotopic Fractionation in the Photochemistry of Nitrate in Water and Ice

J. R. McCabe,* C. S. Boxe, A. J. Colussi ,** M. R. Hoffmann,** M. H. Thiemens***

*Department of Chemistry and Biochemistry, University of California, San Diego, La Jolla, California 92093, and **W. M. Keck Laboratories, California Institute of Technology, Pasadena, CA 91125

In Press: ***Journal of Geophysical Research***

Abstract

We recently reported the first multiple oxygen isotope composition of nitrate (NO_3^-) in ice cores.[1] Post-depositional photolysis and volatilization may alter the isotopic signatures of snowpack nitrate. Therefore, the precise assessment of the geochemical/atmospheric significance of O-isotopic signatures requires information on the relative rates of photolysis ($\lambda > 300$ nm) of $N^{16}O_3^-$, $N^{16}O_2{}^{17}O^-$ and $N^{16}O_2{}^{18}O^-$ in ice. Here we report on ^{17}O- and ^{18}O-fractionation in the 313 nm photolysis of 10 mM aqueous solutions of normal Fisher KNO_3 (i.e., $\Delta^{17}O = -0.2 \pm 0.2$ ‰) and ^{17}O-enriched USGS-35 $NaNO_3$ ($\Delta^{17}O = 21.0 \pm 0.4$ ‰) between -30 and 25 ^oC. We found that Fisher KNO_3 undergoes mass-dependent O-fractionation, i.e., a process that preserves $\Delta^{17}O = 0$. In contrast, $\Delta^{17}O$ in USGS-35 $NaNO_3$ decreased by 1.6 ± 0.4 ‰ and 2.0 ± 0.4 ‰ at 25 ^oC, 1.2 ± 0.4 ‰ and 1.3 ± 0.4 ‰ at -5 ^oC, and 0.2 ± 0.4 ‰ and 1.1 ± 0.4 ‰ at -30 ^oC, after 12 and 24 hours, respectively. Since the small quantum yield (~ 0.2 %) of NO_3^- photodecomposition into (NO_2 + OH) is due to extensive cage recombination of the primary photofragments rather than to intramolecular processes, the observed $\Delta^{17}O$ decreases likely reflect competitive O-isotope exchange of geminate OH-radicals with H_2O ($\Delta^{17}O = 0$) and escape from the solvent cage, in addition to residual O-isotope mixing of the final photoproducts NO, NO_2, NO_2^- with H_2O. At the prevailing low temperatures, photochemical processing will not impair the diagnostic value of O-isotopic signatures in tracing the chemical ancestry of nitrate in polar ice.

Introduction

Recent field studies in Antarctica and Greenland have shown excess levels of NO_x above sunlit snowpacks, suggesting the potential role of photochemistry.[2,3] Several subsequent laboratory studies support this hypothesis and have attempted to quantify the importance of nitrate photolysis as a source of NO_x (NO and NO_2) in the polar troposphere.[4-6] Nitrate photolysis ($\lambda > 295$ nm) proceeds via two primary pathways:

$$NO_3^- + h\nu + H+ \rightarrow NO_2 + OH \quad (1)$$

$$NO_3^- + h\nu \rightarrow NO_2^- + O(^3P) \quad (2)$$

Surface snow has been known to contain up to 300 ng g^{-1} (6.70 μM) of nitrate; however, typical concentrations below 1 meter are only 20-80 ng g^{-1} (0.45-1.78 μM).[7] Mulvaney *et al.*[8] measured surface-veneer snow nitrate concentrations and obtained a mean value of 96 ng g^{-1} (2.14 μM), whereas newly accumulated snow contained 79 ng g^{-1} (1.76 μM). The Vostok nitrate record is a prime example of near-surface increases that have been attributed to post-depositional processes and redistribution within the snowpack.[9] However, the recent increases in concentration at South Pole are attributed to increased denitrification of the stratosphere as a potential source to the snowpack.

The existence of seasonality in the nitrate ice record is well documented and suggests that photochemical transformations may contribute to the observed variations.[8] Major anions, such as Cl^- and SO_4^{2-}, have large oceanic inputs and exhibit seasonal and spatial variability. In contrast, Antarctic nitrate, which has no known oceanic source, shows no difference in surficial concentrations between coastal and inland locations.[10] Although the sources of nitrate to the Antarctic are still not well understood, this feature implies well-mixed sources over the

continent, such as long-range transport from mid-latitudes or denitrification of the Antarctic stratosphere, with subsequent subsidence over the ice sheet.

Nitrate is a major anion in polar ice,[11-13] which is formed in the atmosphere by NO_x oxidation via OH and O_3. Since NO_3^- is the primary sink for atmospheric NO_x, its chemical history provides a key to understanding the global nitrogen budget and the oxidation capacity of the atmosphere over time. Even though ice cores contain chemical concentration and isotopic changes that serve as valuable records of paleoclimate variations, quantitative interpretations of nitrate have proven elusive. Our understanding of variations in ice core nitrate concentrations has been limited by loss processes occurring during depositional and post-depositional periods, associated with temperature, accumulation rate, diffusion, photochemistry and volatilization.[7] However, the relative influence and exact mechanisms of these limiting factors have yet to be fully understood or quantified. For example, while a study of N and O isotopes in Greenland observes little influence from post-depositional fractionation,[14] the interpretation of other isotopic records of $\delta^{15}N$ from Greenland and Antarctic ice core nitrate is attributed primarily to depositional and post-depositional effects providing further evidence for the implicit uncertainty in the global nitrogen budget.[15]

The recent observation of a mass-independent oxygen isotopic composition in atmospheric NO_3^- has offered a new application to paleoclimate studies.[1,16] Mass-independent oxygen, which is produced during ozone formation, was first observed by Thiemens and Heidenreich.[17] Typically, oxygen isotopes fractionate based on diminutive mass differences between isotopomers, which in turn generate small differences in translational velocity and bond strength. This process is quantified by the following equation:

$$\delta^{17}O = 0.52 \text{ x } \delta^{18}O \tag{3}$$

Any deviation from this primary relationship is defined to be a mass-independent effect, which is any non-zero value in the equation:

$$\Delta^{17}O = \delta^{17}O - 0.52 \text{ x } \delta^{18}O. \tag{4}$$

$\delta^{17}O$ and $\delta^{18}O$ signifies the variation in parts per thousand (‰) of the isotopic ratio of a sample (SA) relative to a standard (ST), which is represented in the conventional isotopic notation,

$$\delta^{17}O = \left[\frac{\left(\frac{^{17}O}{^{16}O} \right)_{SA}}{\left(\frac{^{17}O}{^{16}O} \right)_{ST}} - 1 \right] \times 1000 \tag{5}$$

$$\delta^{18}O = \left[\frac{\left(\frac{^{18}O}{^{16}O} \right)_{SA}}{\left(\frac{^{18}O}{^{16}O} \right)_{ST}} - 1 \right] \times 1000 . \tag{6}$$

Numerous atmospheric molecules exhibit a mass-independent effect: CO, N_2O, H_2O_2, SO_4, NO_3, and stratospheric CO_2. The unique advantage of measuring multiple oxygen isotopes ($\delta^{17}O$, $\delta^{18}O$) lies in the high degree of specificity in the identification of sources and transformation processes (see reviews: Thiemens[18] and Thiemens[19]). Atmospheric ozone (O_3) is the source of mass-independent oxygen; therefore, the observation of mass-independent values in atmospheric molecules can be ascribed to the involvement of ozone in their chemical transformations. In the case of NO_3^- deposition, the influence of the atmosphere on the hydrosphere is clearly resolved through the use of $\Delta^{17}O$-NO_3^- measurements.[20] The potential for employing $\Delta^{17}O$-NO_3^- in the

context of paleoclimate studies lies in the ability to define the magnitude of depositional and post-depositional processes, compared to the atmospheric sources of nitrate to the snowpack. We present here an investigation into the degree of isotopic fractionation that occurs via photolysis of both mass-dependent KNO_3 and mass-independent USGS-35 $NaNO_3$ in ice and aqueous phase, which in turn, quantitatively displays the extent that nitrate photochemistry plays as a significant post-depositional loss process.

Experimental Procedure

The experimental setup has been described previously in Boxe *et al*.[4] and Dubowski *et al*.[6] Solutions of 10 mM Fisher KNO_3 and USGS-35 $NaNO_3$ were spray-frozen onto a coldfinger (CF) at -30 ^{o}C; uniform nitrate-doped ice layers were irradiated at specified temperatures. Aqueous-phase photolysis experiments were conducted in the same apparatus, but the bulk solution resided at the bottom of the quartz sheath (QS), rather than the walls of the cold finger. The quartz sheath-coldfinger apparatus was enclosed in a reflective cylinder and irradiated with three, 5-inch long Hg Pen-Ray UV lamps (UVP, modal 90-0001-04) with primary emission at 313 ± 20 nm. The photon flux incident on the QS, $\boldsymbol{I}_i = 1.50 \times 10^{15}$ photons cm^{-2} s^{-1} (~ 0.35 sun equivalents), was determined by potassium ferrioxalate actinometry at 298 K.[21] The stability of the lamp output was monitored with a photocell (UDT Sensors, model PIN UV 100L), covered by a low-density filter; a Keithely 2000 multimeter was connected to the photocell for measuring lamp output. Irradiation was conducted for intervals of 12, 24, and 48 hours for Fisher KNO_3 solutions and 12 and 24 hours for the USGS-35 $NaNO_3$ solutions. Throughout the experiment, 1.5 L/min of UHP (ultra-high purity) He was used as a carrier gas to flush the produced photoproducts from the reaction chamber. Control experiments were carried out by spraying

solutions onto the cold finger and flowing 1.5 L/min of UHP He for 30 min in the absence of irradition.

After irradiation, the nitrate-doped ice was melted and collected. NO_3^- concentrations were measured on a Dionex DX500 Ion Chromatograph with a 5 μL sample loop. The residual post-photolysis nitrate was converted to $AgNO_3$, using a Dionex AMMS-III suppressor column with a 2.5 mM solution of Ag_2SO_4 as regenerant. The solutions were divided into aliquots containing 10 to 25 μmoles and freeze-dried in silver boats for combustion at 520 ± 10 ^oC. The resulting O_2 was analyzed for $\delta^{17}O$ and $\delta^{18}O$ on a Finnigan Mat 251 multiple collector mass spectrometer, using the method described in Michalski *et al*.[22] Three to four replicate analyses were conducted for each irradiation trial.

Results and Discussion

1. Isotope Effects in NO_3^- photolysis

Several studies of mass-independent effects in oxygen and sulfur isotopes have revealed the importance of UV as a source of an anomalous fractionation.[23-25] While these effects originate in the gas-phase, only one study has shown evidence of a small mass-independent fractionation in the solid phase.[26] No work has investigated the potential effects in the aqueous media, containing ions, NO_3^-, SO_4^{2-}, where their formation in the atmosphere has recently been shown to result in mass-independent isotopic compositions. The results of this study revealed a small fractionation effect in $\delta^{18}O$ in the solid phase that was enhanced in the aqueous phase, where $\Delta^{17}O \neq 0$ values, although minute, were observed.

Photolysis of mass-dependent Fisher KNO_3 ($\delta^{18}O$ = 20.2 ± 1.4‰, $\Delta^{17}O$ = -0.2 ± 1.4‰) for 12, 24 and 48 hours, resulted in an oxygen isotopic composition ($\delta^{17}O$ and $\delta^{18}O$) containing a

slope of 0.51 (see Fig 7.1) with no significant change in slope, indicating that the photolysis of NO_3^- is strictly mass-dependent. The corresponding fractionation observed in $\delta^{18}O$ of Fisher KNO_3 and is presented in Figure 7.2a. The resulting enrichment factors for experiments at 18.4, -5, and -30 ^oC were ε = -3.7 ± 2.0 ‰, ε = -1.5 ± 1.1 ‰, ε = -1.8 ± 0.9 ‰, respectively. The $\delta^{18}O$ enrichment factors observed in USGS-35 (see Fig 7.2b) were ε = -8.2 ± 2.3 ‰, ε = -6.3 ± 1.0 ‰, and ε = -3.5± 0.9 ‰, at 25, –5, and –30 ^oC, correspondingly.

The small depletion in the residual heavy isotopes rather than enrichment suggests two possible explanations. First, secondary reactions produced nitrate with an altered isotopic composition through mixing with another depleted reservoir. Second, the observed photo-induced isotopic fractionation effects (PHIFE) are due to ZPE(zero point energy)-shifts that affect the relative absorption spectra for the isotopomers of NO_3^- during photolysis in water and ice.[27] To evaluate the second case, we find that the experimentally observed vibrational spectra of KNO_3 salt isotopomers ($KN^{16}O_3$, $KNO^{16}O_2{}^{17}O$ and $KN^{16}O_2{}^{18}O$) will result in ZPE-shifts that equate to very small blue-shifts in the absorption spectrum of the heavier isotopomers.[28] Based on the absorption cross section of aqueous nitrate between 280 to 360 nm,[29] the result for aqueous nitrate photolysis will be a depletion in $\delta^{18}O$ and $\delta^{17}O$ of the residual nitrate below 302 nm and an enrichment in $\delta^{18}O$ and $\delta^{17}O$ above 302 nm. With 313 nm as our primary emission, we would expect to observe the latter effect. In fact, the present study reveals the opposite -- depletion in the heavy isotopes. Our results are more consistent with the first explanation that suggests formation of secondary nitrate via oxidation by OH and H_2O. Proper evaluation of this interpretation is not possible with $\delta^{18}O$ alone due to the non-linearity observed in the data

(Figure 7.2a & 7.2b). However, the well-constrained $\Delta^{17}O$ data provides a device for more accurate investigation.

The primary motivation for studying photochemical effects of mass-independent USGS-35 $NaNO_3$ ($\delta^{18}O$ = 55.8, $\Delta^{17}O$ = 21.0) is to provide the most accurate representation of the observed isotopic composition in ice cores.[1] Coincidentally, the mass-independent isotope measurements also serve as a better tool to observe the dynamics of the photochemical system. After 24 hours of irradiation, USGS-35 $NaNO_3$ ($\Delta^{17}O$ = 21.0 ‰) displayed a 6.7 ± 1.9% reduction in $\Delta^{17}O$ at -5 ^{o}C, which was amplified to 9.6 ± 1.9% at 25 ^{o}C (Figure 7.3). The larger reduction of $\Delta^{17}O$ observed in the aqueous photolysis experiments, suggests the influence of water ($\Delta^{17}O$ = 0) via aqueous phase oxidation processes. A diminution of $\Delta^{17}O$, although to a lesser extent, in irradiated nitrate in ice lends support for the proposition that nitrate photolysis and its associated chemistry are primarily occurring in a quasi-liquid layer (QLL) surrounding ice crystals.[4,29,30] The photochemical effects of oxygen isotopes in nitrate reveal a complex system governed by a combination of photo-induced isotope fractionation and subsequent oxidation of the photoproducts to produce secondary nitrate. Evidence of these competing effects is observed in Fig 7.2b where 24 hours of irradiation decreased the nitrate concentration 75% with no significant change in $\delta^{18}O$.

2. The Role of Water: Formation of Secondary Nitrate

Irradiation of the mass-independent USGS-35 $NaNO_3$ ($\delta^{18}O$ = 55.8 ± 1.5 ‰, $\Delta^{17}O$ = 21.0 ± 0.4 ‰) for 12 and 24 hours resulted in a small decrease in $\Delta^{17}O$ (see Figure 7.3). However, with no source of mass-independent fractionation (MIF) in the mass-dependent samples, the

explanation must lie elsewhere. As discussed above, the depletion of $\delta^{18}O$ in the residual nitrate suggests the role of secondary reactions and possible, but less likely, photo-induced isotopic fractionation from ZPE-shifts (Zero Point Energy-shifts) in the absorption spectra of NO_3^- isotopologues. In those cases where there is no apparent source of mass-independent fractionation but a change in $\Delta^{17}O$ is observed, there must be isotopic mixing with a source containing a mass-dependent composition. We observe a depletion of $\delta^{18}O$ suggesting the influence of a source with much lower $\delta^{18}O$ composition. In the present case, the source of admixture is likely water. We conducted a second set of experiments in which the isotopic composition of the solvent water was changed. The results yielded a significantly different fractionation effect upon photolysis implicating the influence of the solvent.

A triple isotope plot of the mass-independent photolysis data set (Fig. 7.4) reveals mixing with the mass-dependent line (slope = 0.52) close to $\delta^{18}O = -36.6 \pm 20.0$ ‰, as defined using the intersection point. This extrapolation suggests mixing with a highly depleted source of mass-dependent oxygen. Warneck and Wurzinger[31] have shown that O_2, $O(^3P)$, and O_3 undergo secondary reactions with NO_2^- during photolysis to produce nitrate:

$$O_2 + O(^3P) \rightarrow O_3 \qquad k_3 = 4 \times 10^9\ M^{-1}\ s^{-1} \tag{7}$$

$$O(^3P) + NO_2^- \rightarrow NO_3^- \qquad k_7 = 1.48 \times 10^9\ M^{-1}\ s^{-1} \tag{8}$$

$$O_3 + NO_2^- \rightarrow NO_3^- + O_2 \qquad k_8 = 3.7 \times 10^5\ M^{-1}\ s^{-1} \tag{9}$$

However, $O(^3P)$ and O_3 typically have enriched $\delta^{18}O$ values. Isotopic mixing with water is a plausible explanation because of the rapid exchange between OH and H_2O, which results in $\Delta^{17}O = 0$ for both species.[32] Consequent oxidation of NO_2 or NO via OH or H_2O, as shown in the following aqueous reactions,[33]

$$NO_2 + NO_2 + H_2O \rightarrow NO_3^- + NO_2^- + 2H^+ \qquad k_9 = 1.0 \times 10^8\ M^{-1}\ s^{-1} \qquad (10)$$

$$NO + NO_2 + H_2O \rightarrow 2NO_2^- + 2H^+ \qquad k_{10} = 2.0 \times 10^8\ M^{-1}\ s^{-1} \qquad (11)$$

$$NO + OH \rightarrow NO_2^- + H^+ \qquad k_{11} = 2 \times 10^{10}\ M^{-1}\ s^{-1} \qquad (12)$$

$$NO_2 + OH \rightarrow NO_3^- + H^+ \qquad k_{12} = 1.3 \times 10^9\ M^{-1}\ s^{-1} \qquad (13)$$

should impart mass-dependent oxygen to the residual NO_3^-, thereby decreasing the $\Delta^{17}O$-NO_3^- value. Nitrite produced from reactions (11) and (12) may then proceed via reaction (9) to yield additional nitrate; still, reaction (9) is 3-5 orders of magnitude slower than other considered reactions. Photoproduction of NO_2, O^-, and OH may undergo subsequent cage reactions in the ice lattice to produce nitrate.[6,30] Rapid exchange of OH with H_2O would again be a source of mass dependent oxygen in the product nitrate.

In order to investigate the potential for isotopic mixing with water, the value of $\delta^{18}O$ and $\delta^{17}O$ in the source water were varied for two spray-freezing experiments. In one case, the water used for NO_3^- solutions was spray-frozen on the coldfinger, melted, and measured for its isotopic composition. The resulting value was $\delta^{18}O = -10.0 \pm 0.5$ ‰ and $\delta^{17}O = -5.1 \pm 0.7$ ‰, which is equivalent to the measured value of the Milli-Q water ($\delta^{18}O = -10.0 \pm 0.5$ ‰ and $\delta^{17}O = -5.1 \pm 0.7$ ‰) used for the nitrate solutions. Therefore, it appears that no fractionation of oxygen isotopes in the water occurs upon spray-freezing. The difference between the intercept expected for pure mixing and that observed in Fig. 7.4 is evidence of compounding influences of several processes, including photochemical fractionation and exchange between mass-independent photoproducts O^- and OH with mass dependent H_2O, thereby decreasing the initial $\Delta^{17}O$ value.

A second photolysis experiment was carried out at -5 ^{o}C for 12 and 24 hours, in which the isotopic composition of the water used to prepare the solution was enriched to $\delta^{18}O = 13.9 \pm 0.5$ ‰ and $\delta^{17}O = 7.3 \pm 0.7$ ‰ through evaporation. Measurements of $\delta^{17}O$ and $\delta^{18}O$ in the residual irradiated nitrate produced an increased slope of 0.96 ± 0.27 that intersects the mass dependent line at $\delta^{18}O = 8.7$ ‰ with a range from –64.1 ‰ to 26.2, rather than -36.7 ‰, ranging from –56.8 ‰ to –22.2 ‰, as in the previous experiments. The fractionation of $\delta^{18}O$ was also substantially smaller than before ($\varepsilon = -6.3$ ‰) with an enrichment factor, $\varepsilon = -0.7$ ‰. In addition, the dilution of $\Delta^{17}O$ values shown in Figure 7.3 is significantly smaller than the previous trials at -5 ^{o}C with a more depleted water source. While this small range in $\delta^{18}O$ that is within the standard deviation of our measurements and the linearity of the values ($R^2 = 0.63$) prevent extreme confidence in our extrapolation to the mass-dependent line, these results are consistent with the role of water as the dilution medium for $\Delta^{17}O$, irrespective of the precise intersection with the mass fractionation line. Other processes, such as photo-induced isotopic fractionation, are likely to affect the isotopic composition of nitrate during irradiation, but the present results provide compelling evidence for the role of secondary nitrate formation via water oxidative processes.

The reduced depletion in $\delta^{18}O$ points to mixing with the enriched water source (see Table 7.1 and Figure 7.2b) while fractionation due to mass-dependent photo-induced effects is likely in the positive direction for the residual nitrate. In this particular case, the narrow range in data is apparently the result of a combination of two effects acting in opposite directions to produce nearly no observed change in $\delta^{18}O$ (see Figure 7.4). The reduction in the magnitude of dilution in $\Delta^{17}O$ under the same irradiation conditions is also indicative of mixing with the more enriched

isotope source (see Figure 7.3). Although the statistical difference between the slopes in Figure 7.4 may not be robust, the results provide sufficient evidence to suggest that changing the isotopic composition of the solvent in our system led to observable changes in the resulting photochemical effects under the same experimental conditions. Therefore, the solvent water is an important component controlling the observed isotope effects in our study.

It is apparent that only a small extent (~ 0.2 %) of NO_3^- photodecomposition into (NO_2 + OH) is due to extensive cage recombination of the primary photofragments rather than to intramolecular processes, that is, the low quantum yields of nitrate's primary photolytic pathways also contribute to the decreasing $\Delta^{17}O$. Reported quantum yields for reaction 1 range from ca. 1.88 x 10^{-3} at -30 ^oC to 1.83 x 10^{-2} at 25 ^oC and for reaction 2 range from ca. 6.74 x 10^{-4} at -30 ^oC to 6.23 x 10^{-3} at 25 ^oC (extrapolated to 25 ^oC from Dubowski *et al.*[30] linear regression for $\ln\phi_{NO_2^-}$ vs. 1000/T between 5 and 21 ^oC).

3. Residual Nitrate Concentrations

In addition to the isotopes, we measured the residual nitrate concentrations (shown in Table 7.1) and observe reductions significantly greater than expected from the reported quantum yields for the primary photoproducts of reactions (1) and (2).[29,30] Nitrate's primary photolysis reactions (reactions 1 and 2) govern its bulk concentration at any time, *t*. Expected nitrate concentrations can then be quantified using $d[NO_3^-]/dt = -(\phi_1 j_1 + \phi_2 j_2)[NO_3^-]$, which, after integrating, yields $[NO_3^-] = [NO_3^-]_o \exp[-(\phi_1 j_1 + \phi_2 j_2)t]$. ϕ_1 and ϕ_2 refer to quantum yields for reactions (1) and (2) at a specified temperature, and j_1 and j_2 correspond to the first-order rate constants over $\lambda = 313 \pm 20$ nm, similarly. Assuming the approximation for molecule A(NO_3^-), *j*

$= \int_{\lambda_1}^{\lambda_2} \sigma_A(\lambda,T)\phi(\lambda,T)I(\lambda)d\lambda \approx \sum_i \sigma_A(\lambda_i,T)\phi(\lambda_i,T)I(\lambda_i)\Delta\lambda_i$, j_1 and j_2 were calculated, where σ_A is the extinction coefficient, ϕ is the quantum yield, and I is the actinic flux.[33] Nitrate extinction coefficients (σ_{NO3-}) were extracted from Gaffney *et al*.[34] At 25, -5, and -30 ^{o}C for 12 to 48 hours of irradiation, initial nitrate concentrations are predicted to decrease by 0.76 - 3.0%, 0.06 - 0.26%, and 0.008 - 0.03%, respectively. This anticipated trend is minuscule and opposite compared to our measured residual nitrate concentrations shown in Table 7.1. We speculate that the unaccounted for nitrate loss could be reconciled to some extent by first considering evidence for primary photolytic pathways other than reactions (1) and (2).[35,36] Further work is needed to verify this possibility.

Furthermore, initial nitrate concentrations decreased more drastically in ice versus solution. This effect is counterintuitive, considering that the quantum yields for both primary photolytic pathways (1) and (2) decrease with decreasing temperature over the temperature range of this study. However, despite a 50 –70 % increase in the loss rate in water versus ice, the rate is not significantly different below freezing (based on results presented in Table 7.1). In the case of KNO_3, aqueous phase photolysis at 18.4 ºC results in a 0.11 ± 0.02 mM h^{-1} decrease while ice phase photolysis at –5 ºC and –30 ºC decrease by 0.19 ± 0.06 mM h^{-1} and 0.18 ± 0.02 mM h^{-1}, respectively. The observation of enhanced nitrate loss in ice demands evaluation in light of its relevance to ice core studies.

Based on our experimental conditions, we must first consider the differences in absorption of nitrate in ice and water based on changes in pathlength. While Dubowski *et al*.[6] shows that quantum yields of NO_2^- do not change with ice thickness, we must consider the

possibility that our phase effect is due to the different photolysis environments in our experiments, neglecting that ice and water absorb differently. In the experiment, ice-phase photolyis was conducted by irradiating a thin coating (~0.02cm) of spray-frozen nitrate-doped ice on a coldfinger while liquid-phase photolysis was conducted by irradiating a solution of nitrate residing at the bottom of the quartz sheath. Using the Beer-Lambert law: $I/Io = \exp(-\varepsilon c l)$, where I/Io is the ratio of transmitted to incident light, ε is the molar absorptivity, c is the concentration, and l is the pathlength, we calculate the differences in absorption, I/Io, between phases in our experiment based on changes in pathlength. With $\varepsilon = 7.5\ M^{-1}\ cm^{-1}$, c = 0.010 M, l = 2 cm for liquid and l = 0.02 cm for ice, we find that the ice absorption can increase by 15%. Therefore, the difference in pathlength between experiments does not fully account for the 50 – 70 % enhanced nitrate loss rate in ice. Future actinometric experiments are needed to resolve the differences in absorption between nitrate in ice and water.

Another explanation for the residual nitrate may pertain to the effect of the freezing process on NO_3^- solutions.[37-39] It is well known that during the freezing process most solutes, including nitrates, are rejected from the ice phase.[40-46] This partitioning effect cannot explain this observation, especially considering that nitrate's two primary photolytic pathways exhibit positive temperature dependence and that only specified non-photolytic reactions are accelerated by freezing. Therefore, this mechanism cannot be considered. Further investigation is needed to resolve the possibility of increased photochemical loss of nitrate in ice due to inherent implications for polar ice studies of nitrate.

Conclusions

The primary intent of investigating the photochemical effects on $\Delta^{17}O\text{-}NO_3^-$ was to evaluate the possibility of implementing mass-independent isotopic measurements to improve the interpretation of the nitrate ice core record. The present experiments provide the first isotopic measurements of NO_3^- during photolysis in aqueous solution and ice. We found that photolysis yielded mass-dependent results. The magnitude of the 0.8 to 2.0 ‰ dilution in $\Delta^{17}O$ is small compared to natural samples and should not limit the ability to resolve the chemical history of nitrate in the polar records since variations in $\Delta^{17}O\text{-}NO_3^-$ observed in atmospheric aerosols and ice cores are 20-30 ‰.[1,16,20] Nitrate photochemistry should therefore have little influence (~10%) on the atmospheric mass-independent isotopic composition preserved in snow. However, future field investigations of air-snow isotopic transfer will provide more direct evidence of $\Delta^{17}O\text{-}NO_3^-$ measurements and their ability to possibly quantify the contribution of photochemistry to post-depositional loss of nitrate in snow and/or interpret ice core records. Based on our results, at lower temperatures the effect should have relatively insignificant changes in the oxygen isotopic composition of nitrate throughout the snowpack. At the relevant temperature, -30 °C, a 35.8% decrease in nitrate (see Table 7.1 and Fig 7.3) results in a negligible 0.3 ± 0.4 ‰ decreases in $\Delta^{17}O$. The greatest effect we observe below freezing is a 1.4 ‰ decrease after 70% loss. A model presented by Wolff *et al.*[47] estimates the maximum photochemical loss of nitrate to be 40% at Dome C, a low accumulation site, where the effect would be most significant. Consequently, the oxygen isotope composition of nitrate in ice should preserve any seasonal or long-term atmospheric variability resulting from denitrification or changes in oxidation pathways in agreement with the findings of Hastings *et al.*[14] On the

other hand, we do acknowledge that the timescale of nitrate photolysis in snow-covered regions occur on much longer timescales than our experiments, which ranged from 12 to 48 hours. 48 hours was chosen as an upper limit for irradiating $[NO_3^-]_o$ since it would be depleted, especially in the ice phase, after ca. 2 days in our single solute system and not allow for precise definition of the isotopic fractionation factors.

Furthermore, implications of these results to other applicable environmental systems must be considered. Recently, Michalski *et al*.[20] presented results of $\Delta^{17}O$ measurements of nitrate in surface limnological waters. The present study suggests that the effect on $\Delta^{17}O$-NO_3^- due to photochemistry is most pronounced in the aqueous environment. Therefore, studies of atmospheric nitrate deposition using oxygen isotopes (^{17}O and ^{18}O) may experience as much as a 2.0 per mil reduction in $\Delta^{17}O$ in near surface waters and a corresponding 10% underestimate of the atmospheric contribution of nitrate.

This study also introduces new issues regarding the photochemical effects in the oxygen isotopic composition of aqueous and frozen nitrate solutions. They appear to result from a combination of photochemical fractionations, along with secondary oxidation by OH or water. The observation of the negative, albeit small, enrichment of the residual nitrate $\delta^{18}O$ was unexpected, and has been attributed to secondary chemical reactions. The trend in $\delta^{18}O$ could be interpreted in terms of photochemical effects alone. However, without the presence of a mass-independent source, the decreased $\Delta^{17}O$ values indicate a greater importance of secondary nitrate produced via OH and H_2O oxidation of the photoproducts NO_2, NO_2^-, and NO. This process is also likely since a small extent (~ 0.2 %) of NO_3^- photodecomposition into (NO_2 + OH) is due to

extensive cage recombination of the primary photofragments rather than to intramolecular processes.

Finally, the enhanced nitrate loss in ice photolysis compared to water is unexpected and future studies dedicated towards its resolution could be of importance. The results may derive from dissimilar geometries of nitrate in ice and aqueous media, where nitrate in the ice phase may experience higher photon fluxes. Thus, this phenomenon will be explored extensively in a future study to evaluate this possibility.

Acknowledgements

UCSD gratefully acknowledges the support of the National Science Foundation, Atmospheric Science and Polar Research. The manuscript also benefited from the comments of two anonymous reviewers and input from Greg Michalski, Larry Hernandez, and Subrata Chakraborty.

Fisher KNO_3

Temperature °C	Irradiation Time (hr)	NO_3^- (mM)	$\delta^{18}O$ (‰)	$\delta^{17}O$ (‰)	$\Delta^{17}O$ (‰)
18.4	0.0	10.00	20.5	10.4	-0.3
-5.0	0.0	10.00	20.2	10.3	-0.2
18.4	12	9.41	17.3	8.9	0.0
	24	6.54	16.1	8.3	-0.1
	48	5.19	17.8	9.3	0.0
	24 (no He)	6.43	15.8	7.9	-0.3
-5	12	8.37	18.3	9.4	-0.1
	24	2.39	17.1	8.7	-0.2
	48	1.43	16.5	8.7	0.1
-30	8	7.23	19.2	9.6	-0.3
	24	5.47	19.2	9.6	-0.4
	46	1.04	15.9	8.1	-0.1

USGS-35 $NaNO_3$

Temperature °C	Irradiation Time (hr)	NO_3^- (mM)	$\delta^{18}O$ (‰)	$\delta^{17}O$ (‰)	$\Delta^{17}O$ (‰)
-5	0	10.00	55.4	49.9	21.0
25	12	9.05	48.7	44.7	19.3
	22.5	6.39	50.5	45.1	18.9
-5	12	8.67	54.5	48.1	19.7
	24	3.98	47.8	44.5	19.6
-5*	12	8.19	55.7	49.7	20.8
	24	2.45	55.1	48.8	20.2
-30	12.5	6.42	51.6	47.5	20.7
	24	4.11	49.9	45.8	19.8

Table 7.1. Oxygen isotope values in initial and residual irradiated Fisher KNO_3 and USGS-35 $NaNO_3$. In one case, liquid nitrate was irradiated for 24 hours with no helium flow. The trials with water oxygen isotope composition $\delta^{18}O = 13.9 \pm 0.5$ ‰ are noted with stars (*).

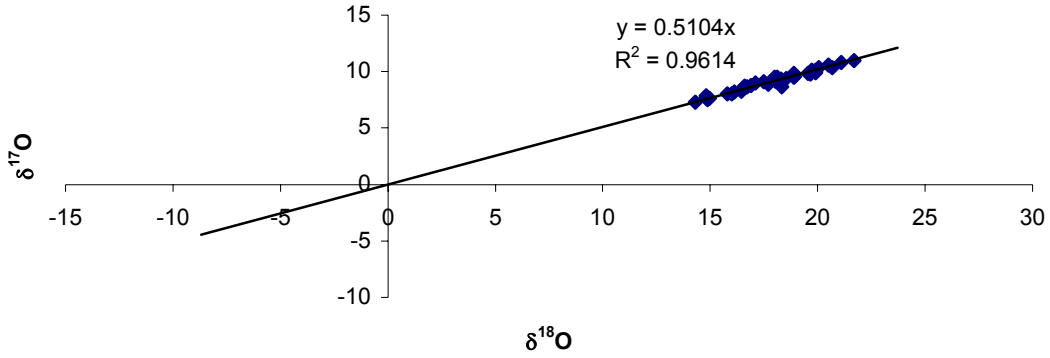

Figure 7.1. $\delta^{17}O$ and $\delta^{18}O$ values in Fisher KNO_3 ($\Delta^{17}O$ = -0.2) after photolysis exhibit mass dependent relationships with a slope of 0.51.

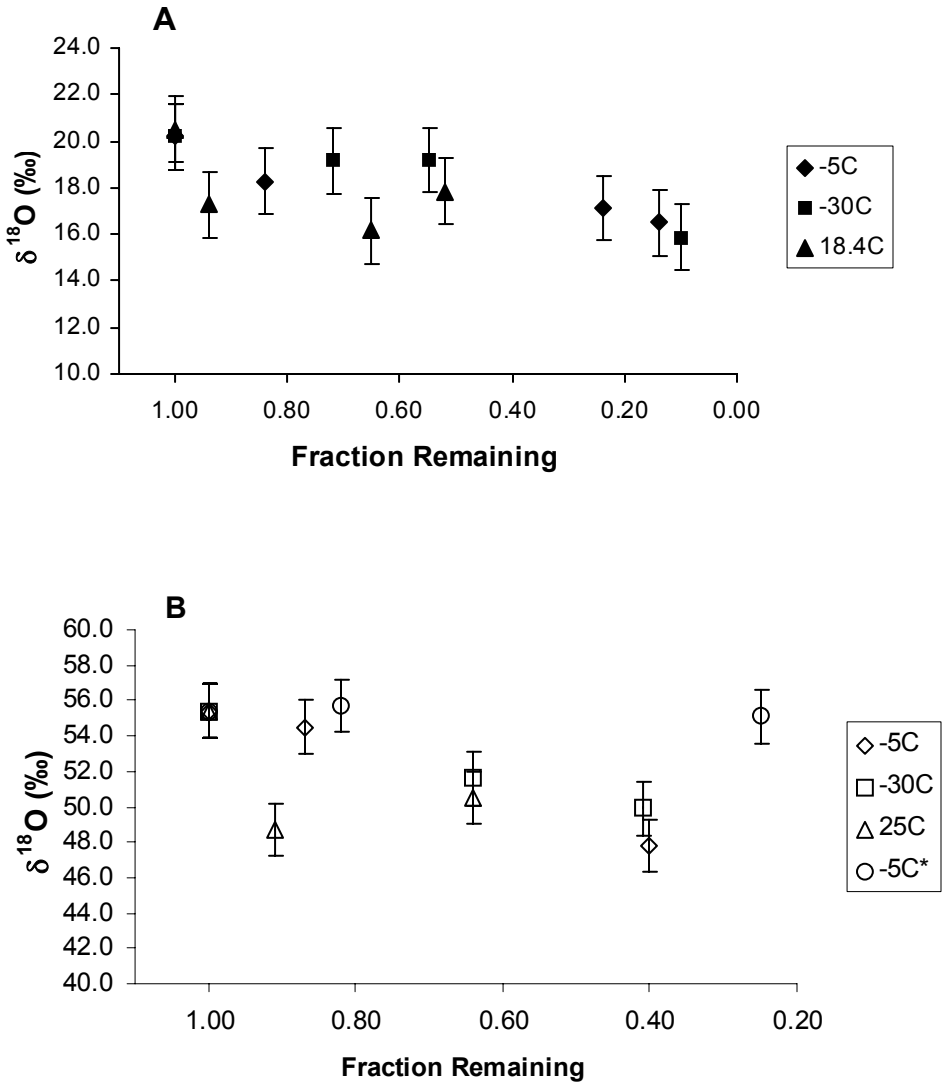

Figure 7.2. Isotopic fractionation of $\delta^{18}O$ vs. remaining fraction of nitrate following photolysis for mass dependent Fisher KNO_3 (A) and mass-independent USGS-35 $NaNO_3$ (B). Concentrations were consistently lower after equivalent irradiation times in ice-doped nitrate experiments at -5 ^{o}C (open and closed diamonds) and -30 ^{o}C (open and closed squares) than aqueous nitrate experiments (open and closed triangles). Experiments conducted with enriched water ($\delta^{18}O$ = 13.9 ‰) are represented as –5 ˚C* and the open circles.

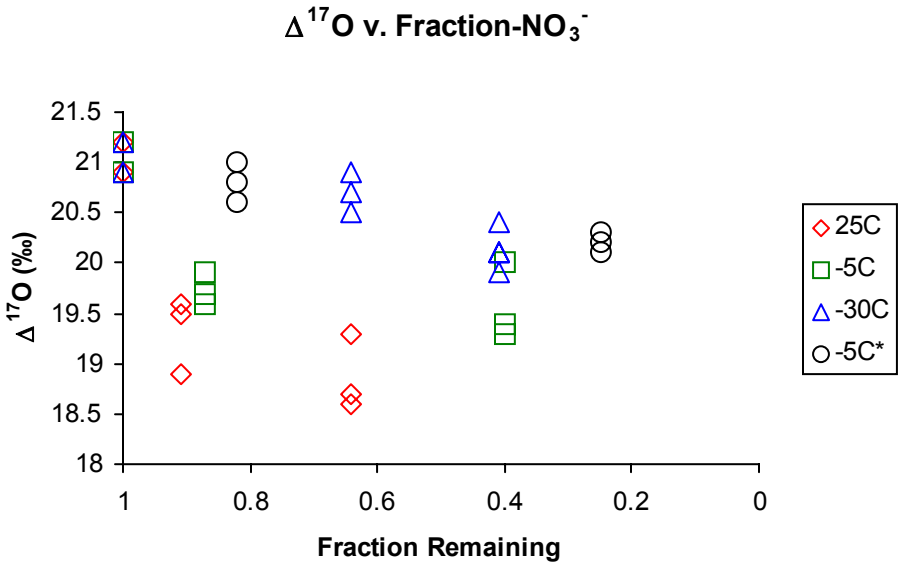

Figure 7.3. Changes in $\Delta^{17}O$ of USGS-35 ($\Delta^{17}O = 21.0 \pm 0.4$ ‰) versus remaining fraction of nitrate after irradiation for 0, 12, and 24 hours. The open circles (-5 ^{o}C*) show the results from USGS-35 irradiation conducted at -5 ^{o}C with solutions of enriched H_2O ($\delta^{18}O = 13.9$ ‰).

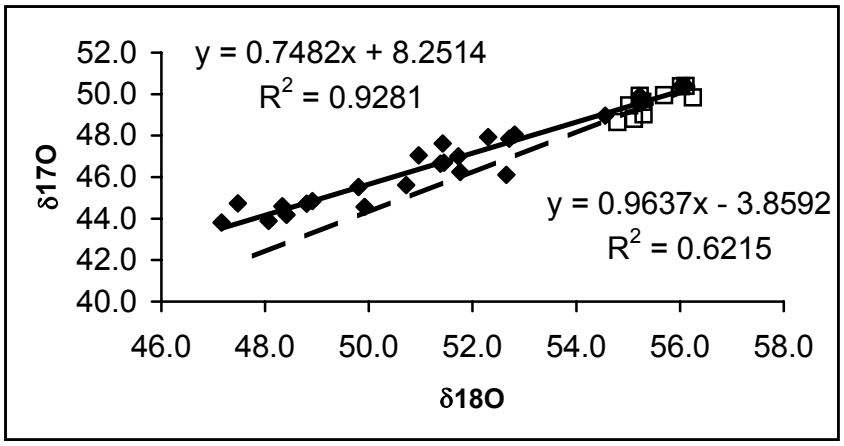

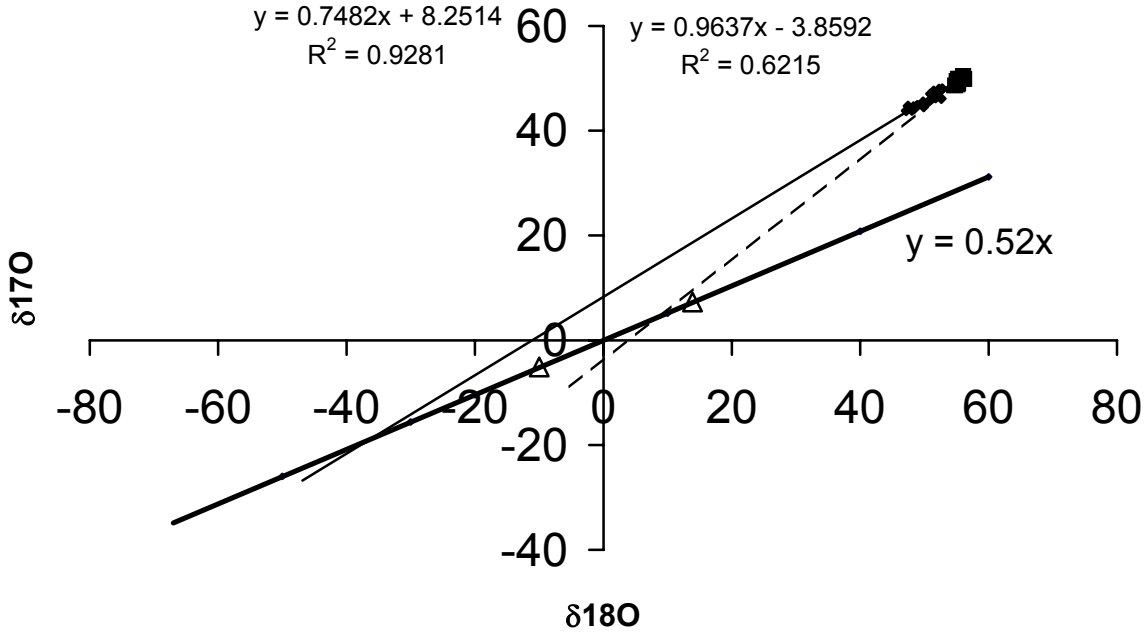

Figure 7.4. $\delta^{17}O$ vs. $\delta^{18}O$ of USGS-35 $NaNO_3$ following irradiation shows evidence of mixing with a depleted mass dependent source. The slope of the initial experimental results when H_2O-$\delta^{18}O$ = -10.0 ‰ is 0.75 ± 0.04, intercepting the mass-dependent line (slope = 0.52) at -36.7 ‰ between –22.2 and –56.8 ‰. A series of trials conducted with solutions using enriched H_2O ($\delta^{18}O$ = 13.9 ± 0.5 ‰) reveal a change in slope to 0.96 ± 0.27 with a more enriched mixing

source (intercept is $\delta^{18}O$ = 8.7 ‰ between –64.1 and 26.2 ‰). The inset shows the range in $\delta^{17}O$ and $\delta^{18}O$ and better resolves the variation in slope between the two experiments. The water oxygen isotope composition of the two cases is represented by the open triangles lying on the bold mass-dependent line (y=0.52x).

References

(1) Alexander, B.; Savarino, J.; Kreutz, K. J.; Thiemens, M. H. *J. Geophys. Res.-Atmos.* **2004**, *109*.

(2) Jones, A. E.; Weller, R.; Wolff, E. W.; Jacobi, H. W. *Geophys. Res. Lett.* **2000**, *27*, 345.

(3) Honrath, R. E.; Peterson, M. C.; Guo, S.; Dibb, J. E.; Shepson, P. B.; Campbell, B. *Geophys. Res. Lett.* **1999**, *26*, 695.

(4) Boxe, C. S.; Colussi, A. J.; Hoffmann, M. R.; Tan, D.; Mastromarino, J.; Case, A. T.; Sandholm, S. T.; Davis, D. D. *J. Phys. Chem. A.* **2003**, *107*, 11409.

(5) Cotter, E. S. N.; Jones, A. E.; Wolff, E. W.; Bauguitte, S. J. B. *J. Geophys. Res.-Atmos.* **2003**, *108*.

(6) Dubowski, Y.; Colussi, A. J.; Hoffmann, M. R. *J. Phys. Chem. A.* **2001**, *105*, 4928.

(7) Wolff, E. W. *Nitrate in Polar Ice*; Springer-Verlag: New York, 1995; Vol. I30.

(8) Mulvaney, R.; Wagenbach, D.; Wolff, E. W. *J. Geophys. Res.* **1998**, *103*, 11021.

(9) Mayewski, P. A.; Legrand, M. R. *Nature* **1990**, *346*, 258.

(10) Mulvaney, R.; Wolff, E. W. *J. Geophys. Res.-Atmos.* **1993**, *98*, 5213.

(11) Dibb, J. E.; Talbot, R. W.; Munger, J. W.; Jacob, D. J.; Fan, S. M. *J. Geophys. Res.* **1998**, *103*, 3475.

(12) De Angelis, D.; Legrand, M. *Ice Core Studies of Global Biogeochemical Cycles, NATO ASI Ser., Ser. 1* **1995**, *30*, 361.

(13) Silvente, E.; Legrand, M. *Ice Core Studies of Global Biogeochemical Cycles, NATO ASI Ser., Ser. 1* **1995**, *30*, 225.

(14) Hastings, M. G.; Steig, E. J.; Sigman, D. M. *J. Geophys. Res.-Atmos.* **2004**, *109*.

(15) Freyer, H. D.; Kobel, K.; Delmas, R. J.; Kley, D.; Legrand, M. R. *Tellus Ser. B-Chem. Phys. Meteorol.* **1996**, *48*, 93.

(16) Michalski, G.; Scott, Z.; Kabiling, M.; Thiemens, M. H. *Geophys. Res. Lett.* **2003**, *30*.

(17) Thiemens, M. H.; Heidenreich, J. E. *Science* **1983**, *219*, 1073.

(18) Thiemens, M. H. *Science* **1999**, *283*, 341.

(19) Thiemens, M. H.; Savarino, J.; Farquhar, J.; Bao, H. M. *Accounts Chem. Res.* **2001**, *34*, 645.

(20) Michalski, G.; Meixner, T.; Fenn, M.; Hernandez, L.; Sirulnik, A.; Allen, E.; Thiemens, M. *Environ. Sci. Technol.* **2004**, *38*, 2175.

(21) Calvert, J.; Pitts, J. N. *Photochemistry*; Wiley: New York, 1966.

(22) Michalski, G.; Savarino, J.; Bohlke, J. K.; Thiemens, M. *Anal. Chem.* **2002**, *74*, 4989.

(23) Savarino, J.; Romero, A.; Cole-Dai, J.; Bekki, S.; Thiemens, M. H. *Geophys. Res. Lett.* **2003**, *30*.

(24) Farquhar, J.; Savarino, J.; Airieau, S.; Thiemens, M. H. *J. Geophys. Res.-Planets* **2001**, *106*, 32829.

(25) Thiemens, M. H.; Jackson, T. *Meteoritics* **1985**, *20*, 775.

(26) Miller, M. F.; Franchi, I. A.; Thiemens, M. H.; Jackson, T. L.; Brack, A.; Kurat, G.; Pillinger, C. T. *Proc. Natl. Acad. Sci. U. S. A.* **2002**, *99*, 10988.

(27) Miller, C. E.; Yung, Y. L. *J. Geophys. Res.-Atmos.* **2000**, *105*, 29039.

(28) Chakraborty, T.; Bajpai, P. K.; Verma, A. L. *J. Raman Spectrosc.* **1999**, *30*, 189.

(29) Chu, L.; Anastasio, C. *J. Phys. Chem. A.* **2003**, *107*, 9594.

(30) Dubowski, Y.; Colussi, A. J.; Boxe, C.; Hoffmann, M. R. *J. Phys. Chem. A.* **2002**, *106*, 6967.

(31) Warneck, P.; Wurzinger, C. *J. Phys. Chem.* **1988**, *92*, 6278.

(32) Meijer, H. A. J.; Li, W. J. *Isot. Environ. Healt. S.* **1998**, *34*, 349.

(33) Sienfeld, J. H.; Pandis, S. N. *Atmospheric Chemistry and Physics*, 1998.

(34) Gaffney, J. S.; Marley, N. A.; Cunningham, M. M. *Environ. Sci. Technol.* **1992**, *26*, 207.

(35) Boxe, C. S.; Colussi, A. J.; Hoffmann, M. R.; Perez, I.; Cohen, R. C. *J. Phys. Chem. A* **2005**.

(36) Madsen, D.; Larsen, J.; Jensen, S. K.; Keiding, S. R.; Thogersen, J. *J. Am. Chem. Soc.* **2003**, *125*, 15571.

(37) Takenaka, N.; Ueda, A.; Daimon, T.; Bandow, H.; Dohmaru, T.; Maeda, Y. *J. Phys. Chem.* **1996**, *100*, 13874.

(38) Takenaka, N.; Ueda, A.; Maeda, Y. *Nature* **1992**, *358*, 736.

(39) Fennema, O. *Water relations of foods*; Academic Press: London, 1975.

(40) Rempel, A. W.; Waddington, E. D.; Wettlaufer, J. S.; Worster, M. G. *Nature* **2001**, *411*, 568.

(41) Killawee, J. A.; Fairchild, I. J.; Tison, J. L.; Janssens, L.; Lorrain, R. *Geochim. Cosmochim. Acta* **1998**, *62*, 3637.

(42) Dash, J. G.; Fu, H. Y.; Wettlaufer, J. S. *Rep. Prog. Physics* **1995**, *58*, 115.

(43) Gross, G. W.; Wong, P. M.; Humes, K. *J. Chem. Phys.* **1977**, *67*, 5264.

(44) Gross, G. W.; McKee, C.; Wu, C. H. *J. Chem. Phys.* **1975**, *62*, 3080.

(45) Gross, G. W. *Adv. Chem. Series* **1968**, 27.

(46) Workman, E. J.; Reynolds, S. E. *Phys. Rev.* **1950**, *78*, 254.

(47) Wolff, E. W.; Jones, A. E.; Martin, T. J.; Grenfell, T. C. *Geophys. Res. Lett.* **2002**, *29*.